Biosensors and Bioelectronics 127 (2019) 142–149

Contents lists available at ScienceDirect

Biosensors and Bioelectronics

journal homepage: www.elsevier.com/locate/bios

A capillary biosensor for rapid detection of *Salmonella* using Fe-nanocluster amplification and smart phone imaging

Huilin Zhang[a], Li Xue[b], Fengchun Huang[b], Siyuan Wang[a], Lei Wang[a], Ning Liu[b], Jianhan Lin[a,b,*]

[a] Key Laboratory of Agricultural Information Acquisition Technology, Ministry of Agriculture and Rural Affairs, China Agricultural University, Beijing 100083, China
[b] Key Laboratory of Modern Precision Agriculture System Integration Research, Ministry of Education, China Agricultural University, Beijing 100083, China

ARTICLE INFO

Keywords:
Capillary biosensor
Fe nanocluster
Prussian Blue
Smartphone APP
Salmonella

ABSTRACT

Early screening of foodborne pathogenic bacteria is a key to prevent and control foodborne diseases. This study intended to develop a capillary biosensor for rapid and sensitive detection of *Salmonella* using the multi-column capillary for easy operation, the Fe-nanoclusters (FNCs) for signal amplification and the smart phone APP for image analysis. The multi-column capillary was successively preloaded the magnetic nanoparticle (MNP) column, the FNC column, two phosphate buffer solution with 0.05% Tween 20 (PBST) columns and the HCl column and the columns were separated by air gap. The iron spiral mixer was fabricated to accelerate the mixing, and the multi-ring magnets was developed to transfer the MNPs and their conjugates from column to column. The target bacteria were captured by the MNPs to form the magnetic bacteria and then conjugated with the FNCs to form the nanocluster bacteria. After washing with PBST, the nanocluster bacteria were transferred into the HCl column, and the iron ions were released and reacted with potassium hexacyanoferrate to form the Prussian Blue, which was finally measured and analyzed using the Hue-Saturation-Lightness color space based smartphone APP for the determination of the target bacteria. This proposed biosensor exhibited a wide linear range for detection of *Salmonella typhimurium* with the lower detection limit of 14 CFU/mL. The mean recovery of the target bacteria in spiked chicken samples was ~105.0%, indicating the applicability of this biosensor. The proposed biosensor had the potential for in-field detection of foodborne pathogens.

1. Introduction

Salmonella, as a major cause of foodborne illness, has attracted great concerns globally (WHO, 2015). Since *Salmonella* is often found in various kinds of foods, the outbreaks of food poisoning caused by *Salmonella* have been occurring worldwide and resulted in significant public health issues and huge economic losses (Procura et al., 2017; Zhang et al., 2018). Rapid screening of the contaminated foods is a key to prevent and control the outbreaks of foodborne diseases. However, the existing methods for bacteria detection, including culture, PCR (Bian et al., 2015; Eigner et al., 2017) and ELISA (Pang et al., 2017; Zhu et al., 2016), either are time-consuming and lab-intensive, or require complex sample pretreatment, or lack sensitivity. Therefore, it is vital to develop rapid, simple and sensitive detection methods to ensure food safety.

In the past decade, various biosensors have emerged as alternatives for rapid detection of foodborne pathogens (Tokonami and Iida, 2017), such as optical biosensors (Kunze et al., 2016; Spehar-Deleze et al., 2016), electrochemical biosensors (Chen et al., 2015; Wang et al., 2017a; Xu et al., 2017; Zhou et al., 2012) and piezoelectric biosensors (Kalograiaki et al., 2016; Ma et al., 2015), etc. These biosensors had shown their merits of high sensitivity, rapid response and/or low cost, however most of them were still at the stage of lab research and required complicated operations, greatly limiting their practical applications. Recently, many efforts have been made to combine biosensing assays with microfluidic platforms for simpler and faster detection of biological targets (de Oliveira et al., 2018; Liu et al., 2017). These microfluidic biosensors could achieve sensitive and automatic detection of biological targets with less human intervention, greatly reducing the operation skill and shortening the detection time. However, at the present stage the microfluidic chips were often fabricated at high cost and with complex procedures, and they also required some sophisticated instrumentation (Jalali et al., 2018; Kant et al., 2018). Besides, some simpler methods using magnetic beads were attempted as well. Bordelon et al. reported an interesting research on a self-contained capillary for nucleic acid extraction using a magnet to transfer the

* Corresponding author at: Key Laboratory of Agricultural Information Acquisition Technology, Ministry of Agriculture and Rural Affairs, China Agricultural University, Beijing 100083, China.
E-mail address: jianhan@cau.edu.cn (J. Lin).

https://doi.org/10.1016/j.bios.2018.11.042

Available online 11 December 2018

magnetic beads from one column to another one, which were preloaded in the capillary (Bordelon et al., 2011). The respiratory syncytial virus RNA could be extracted rapidly and easily with an efficiency of 55%. More importantly, it did not need any instrumentation and had the potential for in-field use.

Signal amplification is a key and challenge issue for biosensors to achieve the desirable sensitivity. In recent years, the protein-inorganic hybrid nanoclusters have been demonstrated to remain and even increase the activity of the enzymes and frequently used as a new approach to amplify biological signals (Altinkaynak et al., 2016; Li et al., 2018; Peng et al., 2018). Another new approach for signal amplification is to utilize the dissolving nanomaterials to release a large amount of metal ions (Kokkinos et al., 2016; Lai et al., 2015; Zhang et al., 2017). Besides, smart phones have become more and more popular in the development of biosensors due to their ubiquity, portability and inexpensiveness (Choi et al., 2016; Wang et al., 2017c). The tailored APP preloaded on the smart phones could be used as image collector and/or data analyzer for biological detection (Zhang and Liu, 2016). Therefore, it might be a promising way to combine these two signal amplification methods with smart phone to develop a simple, sensitive and low-cost biosensor for in-field detection of foodborne pathogens.

In our previous studies, we have developed two double-layer capillary based electrochemical and optical biosensors for the detection of foodborne bacteria (Huang et al., 2017; Wang et al., 2017b). Most procedures, including immunomagnetic separation, enzymatic catalysis and/or fluorescent labeling, were completed in the capillary. Although these biosensors were able to separate the target foodborne bacteria from a large volume of samples with an separation efficiency of ~80% and detect the bacteria as low as 10^1 CFU/mL, the fluidic control was still dependent on the external precise pumps and electronic devices, and this greatly limited their in-field applications since the pumps were prone to suffer the cross-contamination. Furthermore, the mixing efficiency was unsatisfactory because the immune magnetic nanoparticles were fixed in the capillary channel, making the immune reaction between the nanoparticles and the bacteria be solid phase-liquid phase reaction. In this study, we intended to develop a simple, rapid and sensitive biosensor for concentration, separation and detection of *Salmonella* using the immune magnetic nanoparticles for bacteria separation, the immune Fe-nanoclusters for signal amplification and the smart phone for image processing. As shown in Fig. 1, this proposed biosensor mainly included the capillary, where the ion release solution (hydrochloric acid, HCl), the washing solution, the polyclonal antibodies (PAbs) and bovine serum albumin (BSA) modified Fe-nanoclusters (FNCs), and the monoclonal antibodies (MAbs) modified magnetic nanoparticles (MNPs) were successively preloaded and separated by the small air gap, and the APP, which was preloaded on the smart phone. First, the sample containing the target bacteria was injected into the MNP column, and incubated with the MNPs using the iron spiral mixer to form the MNP-bacteria complexes (magnetic bacteria). Then, the magnetic bacteria were transferred into the FNCs column using the multi-ring magnets and incubated with the FNCs to form the MNP-bacteria-FNC complexes (nanocluster bacteria), followed by washing twice with PBST to avoid non-specific binding. After the nanocluster bacteria were transferred into the HCl column, the iron ions (Fe^{3+}) were released from the nanocluster bacteria and reacted with $K_4Fe(CN)_6$ to form the Prussian Blue (PB). Finally, the color of the PB was detected by the imaging APP on the smart phone for quantitative determination of the target bacteria (Scheme 1).

2. Materials and methods

2.1. Materials

The deionized water produced by Millipore Advantage 10 (18.2 MΩ cm, Billerica, MA, USA) was used for preparing all the solutions. The concentrated phosphate buffered saline (PBS) from Sigma-Aldrich (St. Louis, MO, USA) was 1:10 diluted with the deionized water and used as buffer solution. Bovine serum albumin (BSA) from EM Science (Gibbstown, NJ, USA) was prepared in PBS (1.0%, w/v) for blocking of the capillary and preparation of the FNCs. Tween 20 from Amresco (Solon, OH, USA) was 1:2000 diluted with PBS to prepare the washing solution (PBST). The streptavidin modified magnetic nanoparticles with the diameter of ~150 nm from Ocean Nano (MHS-150-10, Dunedin, FL, USA) were used for separation of the target bacteria. The anti-*Salmonella* monoclonal antibodies with the concentration of 1 mg/mL from Abcam (Cambridge, MA, USA) and the anti-*Salmonella* polyclonal antibodies with the concentration of 2.5 mg/mL from Meridian (Memphis, TN, USA) were used for specific reaction with the target bacteria. The long-arm biotin labeling kit from Elabscience Biotechnology (Wuhan, China) was used for the modification of biotin onto the monoclonal antibodies. Ferric chloride from Macklin Biochemical Reagent (Shanghai, China) was used for the synthesis of the protein-inorganic hybrid nanoclusters. Potassium hexacyanoferrate trihydrate from Siaopharm Chemical Reagent (Shanghai, China) was used to form the Prussian Blue.

2.2. Preparation of the bacteria culture

Salmonella typhimurium (ATCC 14028) was used as the target bacteria, while *E. coli* O157:H7 (ATCC 43888) and *Listeria monocytogenes* (ATCC 13932) were used as the non-target bacteria. For bacterial culture, these bacteria were revived by streaking on Luria-Bertani (LB) agar plates and cultured at 37 °C at 180 rpm for 12–14 h, and then serially 10-fold diluted with the sterile PBS to prepare the pure bacteria cultures with the concentrations of 10^1–10^8 CFU/mL.

For bacterial enumeration, the bacterial samples were serially 10-fold diluted with the sterile PBS and 100 μL of the diluents were surface plated on the LB agar plates. The plates were incubated at 37 °C for 22–24 h and the visible colonies were counted for enumeration of the bacteria.

2.3. Preparation of the capillary

The capillary is the most important component in this proposed biosensor. The glass capillary with the inner diameter of 1.8 mm, the outer diameter of 2.0 mm and the length of 300 mm was first blocked by 1% BSA (w/v) for 45 min and washed with PBS. Then, 100 μL of HCl, 100 μL of PBST, another 100 μL of PBST, 100 μL of the FNCs and 10 μL of the MNPs were successively injected into the capillary to form one HCl column, two PBST columns, one FNC column and one MNP column, and ~2 mm of air gap was used to separate each two adjacent columns. The spiral mixer was prepared by filling the iron powder with the size of ~100 μm in a smaller glass spiral capillary (inner diameter: 0.5 mm, outer diameter: 0.6 mm, length: 15 mm) and sealing both ends. The multi-ring magnets were re-designed based on our previous study (Xue et al., 2018) and fabricated by placing 20 ring magnets (grade: N40, material: NdFeB, outer diameter: 5.5 mm, inner diameter: 2.5 mm, thick: 0.5 mm) in mutual attracting layouts in the 3D-printed holder.

2.4. Preparation of the immune MNPs and the immune FNCs

For the preparation of the immune MNPs, the MAbs against *Salmonella* were first labelled with biotin using the biotin labeling kit according to the manufacturer's protocol. After 30 μg of the streptavidin modified MNPs (1 mg/mL) were washed with PBS and resuspended in 500 μL of PBS, 3 μL of the biotinylated MAbs (1 mg/mL) were added and incubated at 15 rpm for 45 min to form the immune MNPs. Then, the MNPs were washed with 500 μL of PBST (PBS with 0.05% Tween 20) to remove the excess MAbs. Finally, the immune MNPs were resuspended in 10 μL of PBS and stored at 4 °C.

For the preparation of the FNCs, the synthesis of the FNCs was slightly modified based on the previously reported method (Ge et al.,

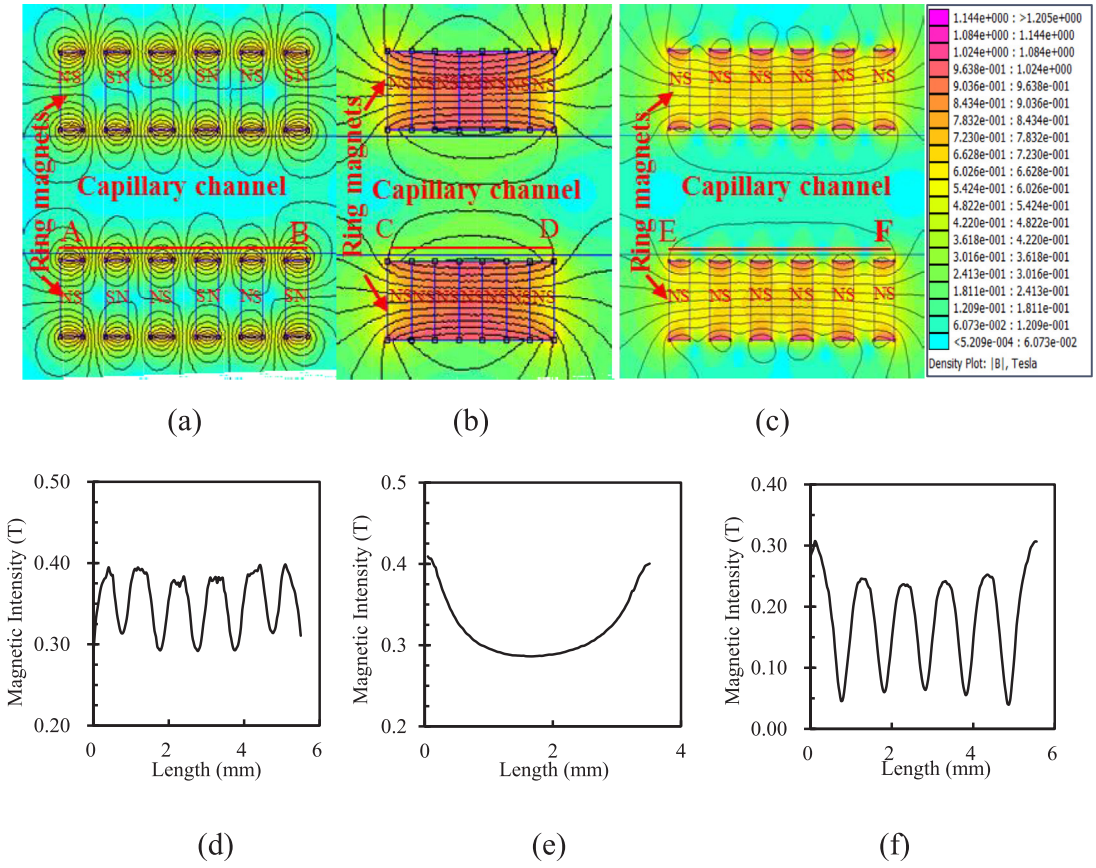

Fig. 1. (a)–(c) The simulation on the distribution of the magnetic field generated by the multi-ring magnets with three different layouts; (d)–(f) the distribution of the magnetic field in the capillary for three layouts.

2012; Li et al., 2016). In brief, 18 μL of the BSA (1 mg/mL) and 8 μL of the PAbs (2.5 mg/mL) were first added into 1 mL of PBS (10 mM, pH 7.4). Then, 100 μL of $FeCl_3$ (100 mM) was added and incubated at 15 rpm for 12 h to form the immune FNCs. To remove the unbound BSA, PAbs and $FeCl_3$, the FNCs were centrifuged at 15,000 rpm for 5 min and washed with the deionized water. After the washing step was repeated, the FNCs were resuspended in 2 mL of the deionized water and stored at 4 °C for further use.

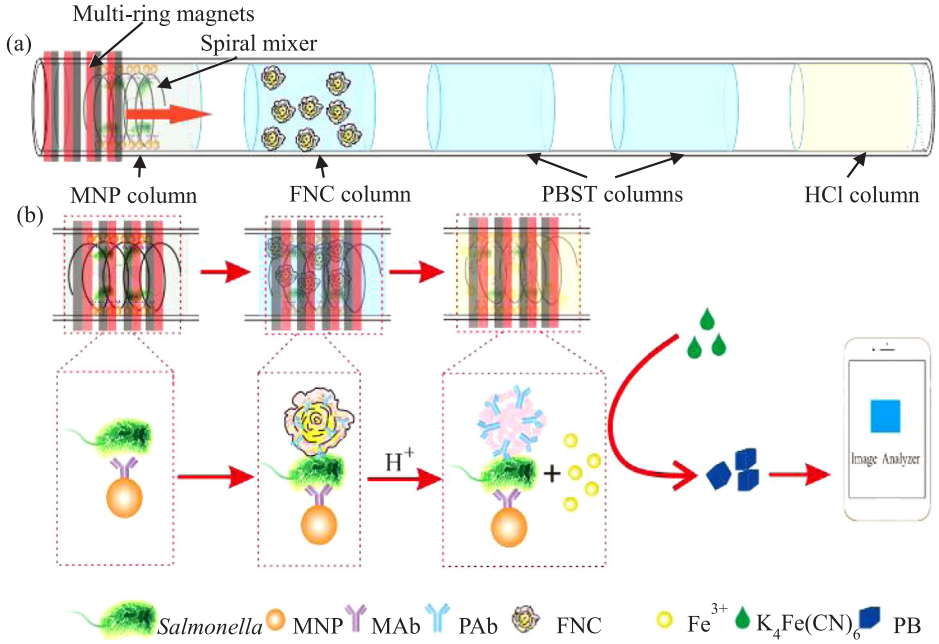

Scheme 1. (a) The capillary successively preloaded with the MNPs, the FNCs, PBST and HCl; (b) the principle of this proposed biosensor for rapid detection of *Salmonella typhimurium*.

2.5. Separation and detection of Salmonella

The separation and detection of the *Salmonella typhimurium* cells were based on the capture of the target bacteria to form the magnetic bacteria in the MNP column, the conjugation of the FNCs with the magnetic bacteria to form the nanocluster bacteria in the FNC column, the washing of the nanocluster bacteria to minimize the non-specific binding in two PBST columns, the release of iron ions to react with $K_4Fe(CN)_6$ to form the PB, and the colorimetric measurement of the PB. First, 100 μL of the sample were injected into the capillary and mixed with the MNPs using the multi-ring magnets to move the spiral mixer forward and backward at 10 mm/s for 45 min to form the magnetic bacteria. Then, the multi-ring magnets were moved towards the FNC column at 2 mm/s, and the magnetic bacteria along with the spiral mixer were transferred into the FNC column. After mixing at 10 mm/s for 45 min, the nanocluster bacteria were formed and washed with the two PBST columns to remove the unbound FNCs using the magnetic field to move forward and backward at 10 mm/s for 3 min. Finally, the nanocluster bacteria were transferred into the HCl column and incubated for 5 min to release Fe^{3+} for reaction with $K_4Fe(CN)_6$ (100 mM) to form the PB. The color of the PB was photographed and analyzed by the imaging APP on the smart phone (Honor 9, Huawei, Shenzhen, China), which was set up ~10 cm above the 96-well plate without external light source, to determine the concentration of the target bacteria. First, the image of the PB was captured using the built-in high-resolution camera. Then, the medium filtering method was used to reduce the background noise and the image was cropped into a 2.5 mm × 2.5 mm square. Finally, the hue value was calculated based on the Hue-Saturation-Lightness (HSL) color space which was converted from the Red-Green-Blue (RGB) color space, and used to determine the amount of the target bacteria in an unknown sample based on the calibration curve between the hue value of the PB and the concentration of *Salmonella typhimurium*.

2.6. Detection of Salmonella in the spiked chicken samples

Twenty-five grams of chicken sample purchased from the local store were first added into 225 mL of PBS and homogenized for 2 min using the stomacher (BagMixer CC, InterScience, Paris, France). Then, 1 mL of different concentrations of *Salmonella typhimurium* were added into 9 mL of the supernatant to prepare the spiked chicken samples with the bacterial concentration ranging from 3.0×10^2 to 3.0×10^6 CFU/mL. Finally, the spiked samples were detected using the proposed biosensor.

3. Results and discussion

3.1. Simulation of the magnetic field

The magnetic field generated by the multi-ring magnets has great impact on the capture of the MNPs and their conjugates and the control of the spiral mixer, which are both important to the proposed biosensor. Thus, the Finite Element Method Magnetics software was used for simulation of different layouts of the multi-ring magnets to find the best design of the magnetic field. As shown in Fig. 1(a), the multi-ring magnets were laid out with all the adjacent magnets repelling each other, which had been reported in our previous study (Xue et al., 2018). Fig. 1(d) showed that this magnetic field had a mean magnetic intensity of ~0.35 T and a mean magnetic gradient of ~67 T/m at the inner wall of the capillary (A-B line). The MNPs and their conjugates could be captured against the inner wall of the capillary and distributed uniformly. However, the magnetic forces applied on the MNPs due to the presence of the multi-ring magnets were mainly vertical to the wall of the capillary, resulting in more difficulty of transferring the MNPs or their conjugates from the first column to the final column due to the additional friction forces. As shown in Fig. 1(b), the multi-ring magnets were laid out with all the adjacent magnets attracting each other without gap. Fig. 1(e) showed that this magnetic field had the same mean magnetic intensity of ~0.30 T and a mean gradient of ~100 T/m at the inner wall of the capillary (C-D line). However, the magnetic field was distributed like U-shape and the magnetic field lines were parallel with the capillary, the MNPs and their conjugates would be captured at both ends of the multi-ring magnets. The magnetic forces on the MNPs were horizontal to the parallel and this would help the MNPs and their conjugates to pass the air gap between two adjacent columns, however the concentrated MNPs could not effectively capture the target bacteria. As shown in Fig. 1(c), the multi-ring magnets were laid out with all the adjacent magnets attracting each other with a 0.5 mm-thick gap. Fig. 1(f) showed that this magnetic field had a smaller mean magnetic intensity of ~0.18 T but a much larger mean gradient of ~400 T/m, which was stronger than the former two layouts. Fig. S1 showed the distribution of the magnetic field in the cross-section capillary from e to f. The mean magnetic intensity and the mean gradient is 0.1 T and 100 T/m, respectively. More importantly, the magnetic forces were exerted on the MNPs and their conjugates in both horizontal and vertical directions, indicating that the MNPs and their conjugates could be captured and distributed in the capillary uniformly, and also could be transferred from column to column easily. Therefore, the third layout with 20 ring magnets was used to set up the multi-ring magnets.

3.2. Quantitative detection of Prussian blue using the smartphone APP

The proposed biosensor was based on quantitative detection of the PB using the smartphone APP for image analysis. To verify the color change of the PB, different different concentrations from 1 to 5 mM were prepared. Their images were collected using the APP and analyzed to obtain their hue values, respectively. Three parallel experiments were conducted for each concentration of the PB. As shown in Fig. 2, a good linear relationship between the hue value (***H***) and the concentration (***C***) of the PB was found and could be described as $\boldsymbol{H} = 11.07 * \ln(\boldsymbol{C}) + 134.31$ ($R^2 = 0.99$). This indicated that the smartphone APP could be used for quantitative determination of the color of the PB at different concentrations from 39 μM to 5 mM. Furthermore, we tested the hue value for different dilution times of FNCs and the results were shown in Fig. S2. Combining Fig. 2 and Fig. S2, it could be estimated that the concentration of Fe^{3+} in FNCs was around 1.881 mM.

3.3. Optimization of the proposed biosensor

The amount of the MNPs played an important role in the bacteria separation and was optimized using the separation efficiency to evaluate the performance. Different amounts (20 μg, 30 μg, 40 μg and 50 μg) of the MNPs were used for separating the *Salmonella typhimurium* cells at the concentration of 3.4×10^4 CFU/mL. The bacteria samples

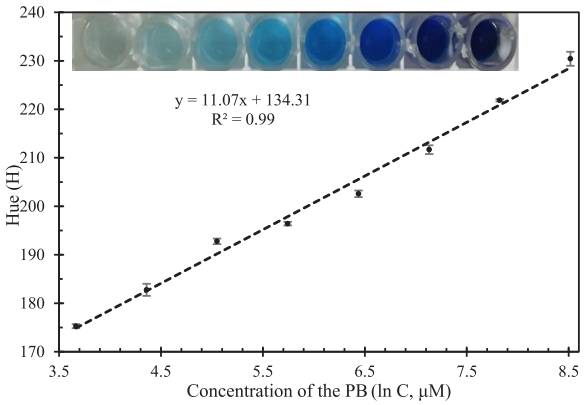

Fig. 2. The hue value for different concentrations of the PB from 39 μM to 5 mM.

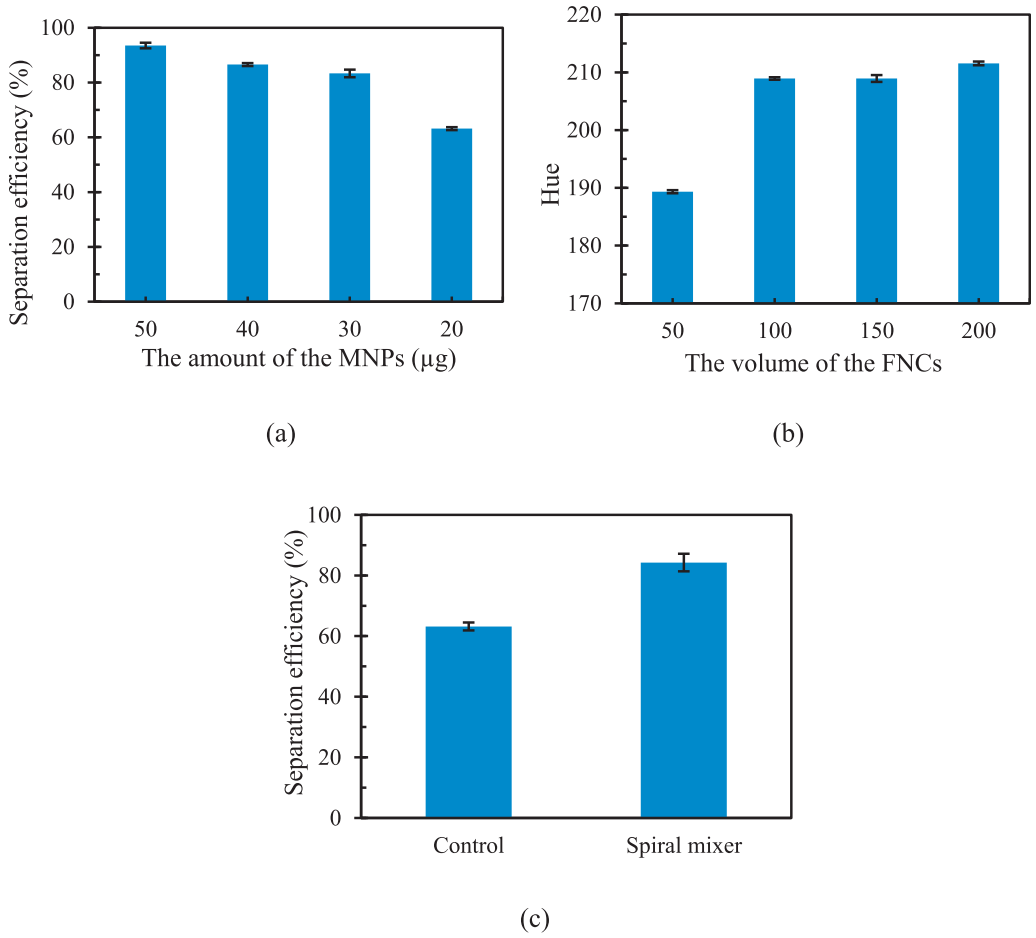

Fig. 3. (a) Optimization of the amount of the immune MNPs (N = 3); (b) optimization of the volume of the immune FNCs (N = 3); (c) comparison of the separation with and without the spiral mixer (N = 3).

before and after separation were enumerated using culture plating. The separation efficiency (SE) was calculated as

$$SE = Ns/Nc \times 100\%$$

where, *Nc* is the concentration of the bacteria before separation; *Ns* is the concentration of the bacteria after separation. As shown in Fig. 3(a), the separation efficiency increased from 63% to 83% when the amount of the MNPs increased from 20 μg to 30 μg. However, when the amount of the MNPs kept increasing to 40 μg and 50 μg, the separation efficiency did not change significantly, indicating that 30 μg was sufficient to capture the target bacteria in the capillary. Thus, the optimal amount of 30 μg for the MNPs was used in this study.

The amount of the FNCs were another key to the sensitivity of the proposed biosensor. Different volumes of the FNCs (50 μL, 100 μL, 150 μL and 200 μL) were used to detect *Salmonella typhimurium* at the concentration of 1.0×10^6 CFU/mL. As shown in Fig. 3(b), the hue value increased from 189.3 to 208.9, when the volume of the FNCs changed from 50 μL to 100 μL. However, when the volume of the FNCs continued increasing to 150 μL and 200 μL, the hue values did not change obviously, indicating that 100 μL of the FNCs were sufficient to react with the target bacteria. Thus, the optimal volume of 100 μL for the FNCs was used in this study.

Besides, the immune reaction between the target bacteria and the MNPs/FNCs is vital to the forming of the MNP-bacteria-FNC complexes and has great impact on the sensitivity of the proposed biosensor. A key to the immune reaction is the complete mixing of the MNPs and the target bacteria, and the magnetic bacteria and the FNCs. Therefore, the spiral mixer was fabricated and used for mixing the MNPs and the target bacteria at the concentration of 3.4×10^4 CFU/mL in the capillary, and the separation efficiency of the bacteria was used to evaluate the mixing performance. As shown in Fig. 3(c), the separation efficiency of the target bacteria without the mixer (used as control) was 63%, however that with the mixer significantly increased to 84%. This was because the reaction between the MNPs and the bacteria mainly relied on the diffusion of the bacteria at the absence of the mixer, resulting in a longer time to achieve the complete reaction, however the moving spiral mixer could greatly enhance the diffusion of the bacteria to improve the reaction efficiency. Thus, the spiral mixer was used in this study.

3.4. Detection of Salmonella typhimurium using the proposed biosensor

Under the optimal conditions, three parallel tests on different concentrations of pure *Salmonella typhimurium* ranging from 3.0×10^2 CFU/mL to 3.0×10^6 CFU/mL were conducted using this proposed biosensor. As shown in Fig. 4, the color of the PB obviously changed from light blue to dark blue when the concentration of *Salmonella typhimurium* increased from 3.0×10^2 CFU/mL to 3.0×10^6 CFU/mL. The color of the PB was measured by the smartphone APP for image analysis to obtain their hue values. As shown in Fig. 4(a), the hue value (***H***) was found to have a good linear relationship with the concentration (***C***) of *Salmonella typhimurium*, and the calibration curve could be described as $\boldsymbol{H} = 2.64 * \lg(\boldsymbol{C}) + 170.63$ ($R^2 = 0.97$). Besides, transmission electron microscope (TEM) was conducted to verify the forming of the MNP-bacteria-FNC complexes, and the TME images of the complexes and the FNCs could be seen in Fig. 4(b–c). According to 3 times of signal-to-noise ratio, the lower detection limit of this proposed biosensor was calculated to be 1.4×10^1 CFU/mL.

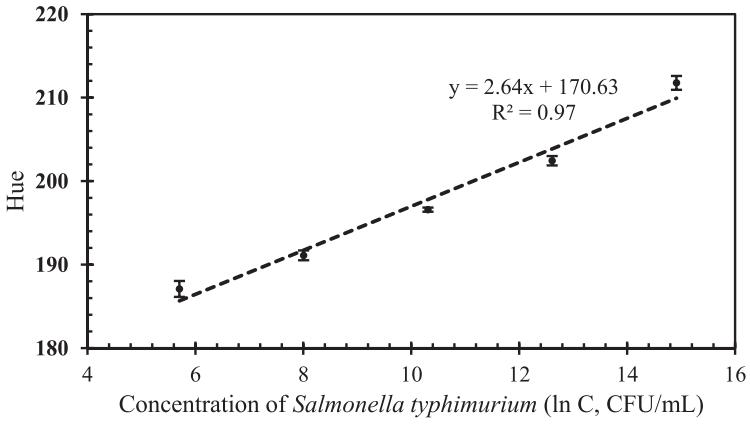

(a)

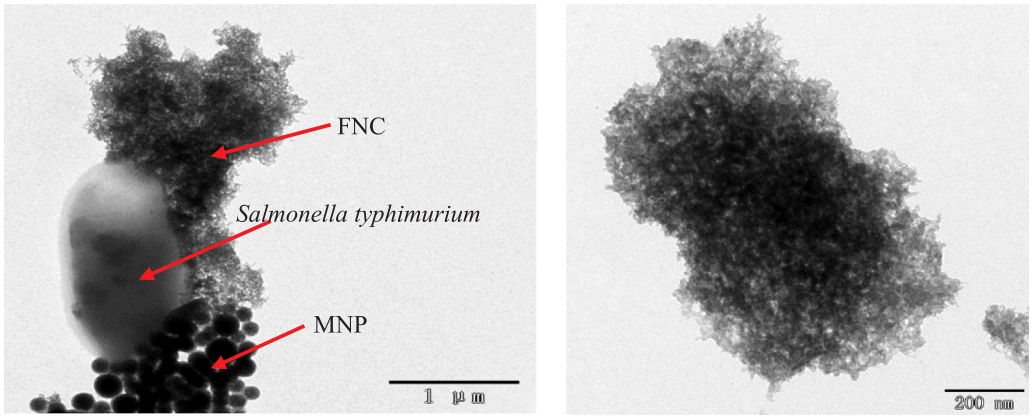

(b) (c)

Fig. 4. (a) Calibration model of this biosensor for detection of *Salmonella typhimurium* ranging from 10^2 CFU/mL to 10^6 CFU/mL; (b) TEM image of the MNP-bacteria-FNC complex; (c) TEM image of the FNC.

3.5. Detection of Salmonella typhimurium in the spiked chicken samples

Three parallel tests on different concentrations of *Salmonella typhimurium* were conducted in the spiked chicken samples to evaluate the applicability of the proposed biosensor. First, the chicken meats purchased from the local supermarket were added into PBS (weight : volume = 1:10) and homogenized for 3 min to obtain the supernatant of the chicken samples. Then, the pure *Salmonella typhimurium* cells were added into the supernatant to prepare the spiked samples containing the target bacteria with different concentrations ranging from 3.0×10^2 CFU/mL to 3.0×10^6 CFU/mL. Finally, the spiked samples were detected using this proposed biosensor and the recovery was calculated to evaluate this biosensor by dividing the number of the bacterial cells obtained from this biosensor by that spiked into the chicken samples. As shown in Fig. 5(a), the hue value increased when the concentration of the *Salmonella typhimurium* cells increased. The recoveries for the target bacteria with the concentrations of 3.0×10^2 CFU/mL, 3.0×10^3 CFU/mL, 3.0×10^4 CFU/mL, 3.0×10^5 CFU/mL and 3.0×10^6 CFU/mL were 111.8%, 107.0%, 99.4%, 107.8%, and 102.3%, respectively, and the mean recovery was 105.7%. Most hue values of the spiked samples were slightly more than those of the pure cultures at the same concentration might be due to the interference of the impurities, such as fat or protein, from the chicken sample background, resulting in more non-specific adsorption and more produced PB. Besides, the hue value had a good linear relationship with the concentration of *Salmonella* ranging from 3×10^2 CFU/mL to 3×10^6 CFU/mL in the chicken samples, which could be described as $\boldsymbol{H} = 2.61 * \lg(\boldsymbol{C}) + 172.23$ ($R^2 = 0.98$), verifying the feasibility of the proposed biosensor for detection of *Salmonella typhimurium* in the chicken samples.

In this study, *Salmonella typhimurium* was used as target bacteria while *Listeria monocytogenes* and *Escherichia coli O157:H7* were used as non-target bacteria to test the specificity of this proposed biosensor. The similar concentration ($\sim 3 \times 10^6$ CFU/mL) of these three bacteria and the negative controls (PBS) were detected using this proposed biosensor. As shown in Fig. 5(b), the hue value for PBS was slightly higher than those of the non-target bacteria, but much lower than that of the target bacteria. This indicated that this developed biosensor had a good specificity.

4. Conclusions

In this study, a simple, rapid and sensitive biosensor for detection of *Salmonella Typhimurium* were successfully developed using the multi-column capillary and the smart phone imaging APP. Under the optimal conditions, this biosensor exhibited a good linear detection range from 3.0×10^2 to 3.0×10^6 CFU/mL of *Salmonella typhimurium* with the lower detection limit of 14 CFU/mL. This proposed biosensor had shown the potential for rapid, sensitive and in-field detection of food-borne pathogens. However, it still has some limitations including (1) the volume of the sample is still very limited and not suitable for detection of target bacteria in a large volume, and (2) the glass capillary is

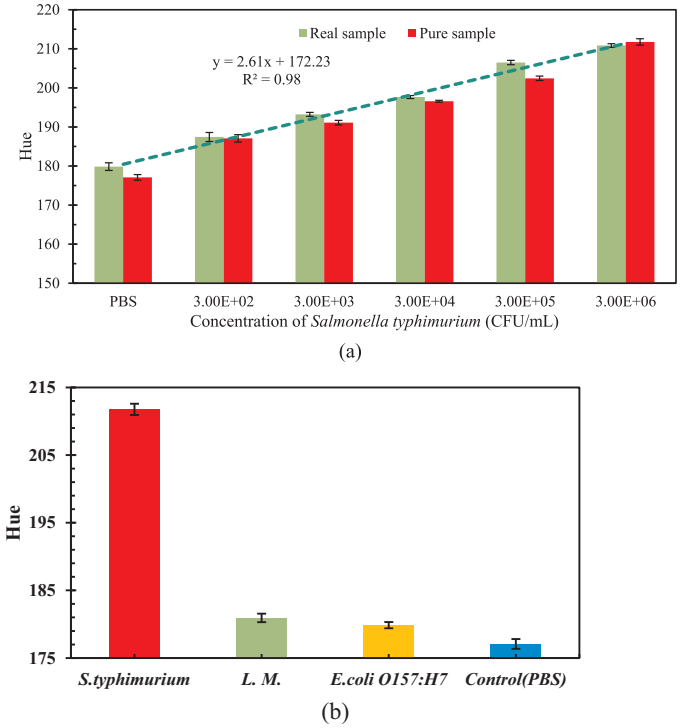

Fig. 5. (a) Detection of *Salmonella typhimurium* with the concentrations from 3.0×10^2 to 3.0×10^6 CFU/mL in spiked chicken samples (N = 3); (b) detection of *Listeria monocytogenes*, *E. coli* O157:H7 and *Salmonella typhimurium* at the same concentration of 3.0×10^6 CFU/mL, and the negative controls (PBS).

too frangible and needs to be handled very carefully.

Acknowledgments

This study was supported in part by the National Natural Science Foundation of China (31802219), Walmart Foundation (SA1703161) and Walmart Food Safety Collaboration Center.

Appendix A. Supporting information

Supplementary data associated with this article can be found in the online version at https://doi.org/10.1016/j.bios.2018.11.042.

References

Altinkaynak, C., Tavlasoglu, S., Ozdemir, N., Ocsoy, I., 2016. A new generation approach in enzyme immobilization: organic-inorganic hybrid nanoflowers with enhanced catalytic activity and stability. Enzyme Microb. Technol. 93–94, 105–112.

Bian, X., Jing, F., Li, G., Fan, X., Jia, C., Zhou, H., Jin, Q., Zhao, J., 2015. A microfluidic droplet digital PCR for simultaneous detection of pathogenic Escherichia coli O157 and Listeria monocytogenes. Biosens. Bioelectron. 74, 770–777.

Bordelon, H., Adams, N.M., Klemm, A.S., Russ, P.K., Williams, J.V., Talbot, H.K., Wright, D.W., Haselton, F.R., 2011. Development of a low-resource RNA extraction cassette based on surface tension valves. ACS Appl. Mater. Interfaces 3 (6), 2161–2168.

Chen, Q., Lin, J., Gan, C., Wang, Y., Wang, D., Xiong, Y., Lai, W., Li, Y., Wang, M., 2015. A sensitive impedance biosensor based on immunomagnetic separation and urease catalysis for rapid detection of Listeria monocytogenes using an immobilization-free interdigitated array microelectrode. Biosens. Bioelectron. 74, 504–511.

Choi, J., Gani, A.W., Bechstein, D.J.B., Lee, J.R., Utz, P.J., Wang, S.X., 2016. Portable, one-step, and rapid GMR biosensor platform with smartphone interface. Biosens. Bioelectron. 85, 1–7.

de Oliveira, T.R., Martucci, D.H., Faria, R.C., 2018. Simple disposable microfluidic device for Salmonella typhimurium detection by magneto-immunoassay. Sens. Actuators B: Chem. 255, 684–691.

Eigner, U., Hiergeist, A., Veldenzer, A., Rohlfs, M., Schwarz, R., Holfelder, M., 2017. Evaluation of a new real-time PCR assay for the direct detection of diarrheagenic Escherichia coli in stool specimens. Diagn. Microbiol. Infect. Dis. 88 (1), 12.

Ge, J., Lei, J., Zare, R.N., 2012. Protein-inorganic hybrid nanoflowers. Nat. Nanotechnol. 7 (7), 428–432.

Huang, F., Zhang, H., Wang, L., Lai, W., Lin, J., 2017. A sensitive biosensor using double-layer capillary based immunomagnetic separation and invertase-nanocluster based signal amplification for rapid detection of foodborne pathogen. Biosens. Bioelectron. 100, 583–590.

Jalali, M., AbdelFatah, T., Mahshid, S.S., Labib, M., Sudalaiyadum Perumal, A., Mahshid, S., 2018. A hierarchical 3D nanostructured microfluidic device for sensitive detection of pathogenic bacteria. Small e1801893.

Kalograiaki, I., Euba, B., Proverbio, D., Campanero-Rhodes, M.A., Aastrup, T., Garmendia, J., Solis, D., 2016. Combined bacteria microarray and quartz crystal microbalance approach for exploring glycosignatures of nontypeable aemophilus influenzae and recognition by host lectins. Anal. Chem. 88 (11), 5950–5957.

Kant, K., Shahbazi, M.A., Dave, V.P., Ngo, T.A., Chidambara, V.A., Than, L.Q., Bang, D.D., Wolff, A., 2018. Microfluidic devices for sample preparation and rapid detection of foodborne pathogens. Biotechnol. Adv. 36 (4), 1003–1024.

Kokkinos, C., Angelopoulou, M., Economou, A., Prodromidis, M., Florou, A., Haasnoot, W., Petrou, P., Kakabakos, S., 2016. Lab-on-a-membrane foldable devices for duplex drop-volume electrochemical biosensing using quantum dot tags. Anal. Chem. 88 (13), 6897–6904.

Kunze, A., Dilcher, M., Abd El Wahed, A., Hufert, F., Niessner, R., Seidel, M., 2016. On-chip isothermal nucleic acid amplification on flow-based chemiluminescence microarray analysis platform for the detection of viruses and bacteria. Anal. Chem. 88 (1), 898–905.

Lai, H.Z., Wang, S.G., Wu, C.Y., Chen, Y.C., 2015. Detection of Staphylococcus aureus by functional gold nanoparticle-based affinity surface-assisted laser desorption/ionization mass spectrometry. Anal. Chem. 87 (4), 2114–2120.

Li, M., Luo, M., Li, F., Wang, W., Liu, K., Liu, Q., Wang, Y., Lu, Z., Wang, D., 2016. Biomimetic copper-based inorganic–protein nanoflower assembly constructed on the nanoscale fibrous membrane with enhanced stability and durability. J. Phys. Chem. C 120 (31), 17348–17356.

Li, Y., Xie, G., Qiu, J., Zhou, D., Gou, D., Tao, Y., Li, Y., Chen, H., 2018. A new biosensor based on the recognition of phages and the signal amplification of organic-inorganic hybrid nanoflowers for discriminating and quantitating live pathogenic bacteria in urine. Sens. Actuators B: Chem. 258, 803–812.

Liu, D., Li, X., Zhou, J., Liu, S., Tian, T., Song, Y., Zhu, Z., Zhou, L., Ji, T., Yang, C., 2017. A fully integrated distance readout ELISA-Chip for point-of-care testing with sample-in-answer-out capability. Biosens. Bioelectron. 96, 332–338.

Ma, F., Rehman, A., Liu, H., Zhang, J., Zhu, S., Zeng, X., 2015. Glycosylation of quinone-fused polythiophene for reagentless and label-free detection of E. coli. Anal. Chem. 87 (3), 1560–1568.

Pang, B., Zhao, C., Li, L., Song, X., Xu, K., Wang, J., Liu, Y., Fu, K., Bao, H., Song, D., 2017. Development of a low-cost paper-based ELISA method for rapid Escherichia coli O157:H7 detection. Anal. Biochem. 542, 58–62.

Peng, T., Wang, J., Zhao, S., Xie, S., Yao, K., Zheng, P., Wang, S., Ke, Y., Jiang, H., 2018. A fluorometric clenbuterol immunoassay based on the use of organic/inorganic hybrid nanoflowers modified with gold nanoclusters and artificial antigen. Mikrochim. Acta 185 (8), 366.

Procura, F., Bueno, D.J., Bruno, S.B., Rogé, A.D., 2017. Prevalence, antimicrobial resistance profile and comparison of methods for the isolation of salmonella in chicken liver from Argentina. Food Res. Int.

Spehar-Deleze, A.M., Julich, S., Gransee, R., Tomaso, H., Dulay, S.B., O'Sullivan, C.K.,

2016. Electrochemiluminescence (ECL) immunosensor for detection of Francisella tularensis on screen-printed gold electrode array. Anal. Bioanal. Chem. 408 (25), 7147–7153.
Tokonami, S., Iida, T., 2017. Review: novel sensing strategies for bacterial detection based on active and passive methods driven by external field. Anal. Chim. Acta 988, 1–16.
Wang, D., Chen, Q., Huo, H., Bai, S., Cai, G., Lai, W., Lin, J., 2017a. Efficient separation and quantitative detection of Listeria monocytogenes based on screen-printed interdigitated electrode, urease and magnetic nanoparticles. Food Control 73, 555–561.
Wang, L., Huang, F., Cai, G., Yao, L., Zhang, H., Lin, J., 2017b. An electrochemical aptasensor using coaxial capillary with magnetic nanoparticle, urease catalysis and PCB electrode for rapid and sensitive detection of Escherichia coli O157:H7. Nanotheranostics 1 (4), 403–414.
Wang, L.J., Chang, Y.C., Sun, R., Li, L., 2017c. A multichannel smartphone optical biosensor for high-throughput point-of-care diagnostics. Biosens. Bioelectron. 87, 686–692.
WHO, 2015. Food Saf. 〈http://www.who.int/mediacentre/factsheets/fs399/en/〉.
Xu, M., Wang, R., Li, Y., 2017. Electrochemical biosensors for rapid detection of Escherichia coli O157:H7. Talanta 162, 511–522.
Xue, L., Zheng, L., Zhang, H., Jin, X., Lin, J., 2018. An ultrasensitive fluorescent biosensor using high gradient magnetic separation and quantum dots for fast detection of foodborne pathogenic bacteria. Sens. Actuators B Chem. 265.
Zhang, D., Liu, Q., 2016. Biosensors and bioelectronics on smartphone for portable biochemical detection. Biosens. Bioelectron. 75, 273–284.
Zhang, Q., Li, L., Qiao, Z., Lei, C., Fu, Y., Xie, Q., Yao, S., Li, Y., Ying, Y., 2017. Electrochemical conversion of Fe3O4 magnetic nanoparticles to electroactive prussian blue analogues for self-sacrificial label biosensing of avian influenza virus H5N1. Anal. Chem. 89 (22), 12145–12151.
Zhang, Z., Wang, Q., Han, L., Du, S., Yu, H., Zhang, H., 2018. Rapid and sensitive detection of Salmonella typhimurium based on the photothermal effect of magnetic nanomaterials. Sens. Actuators B: Chem. 268, 188–194.
Zhou, L., Li, D.-J., Gai, L., Wang, J.-P., Li, Y.-B., 2012. Electrochemical aptasensor for the detection of tetracycline with multi-walled carbon nanotubes amplification. Sens. Actuators B: Chem. 162 (1), 201–208.
Zhu, L., He, J., Cao, X., Huang, K., Luo, Y., Xu, W., 2016. Development of a double-antibody sandwich ELISA for rapid detection of Bacillus Cereus in food. Sci. Rep. 6, 16092.